Collisionality dependence of the quasilinear particle flux due to microinstabilities

T. Fülöp,[1] I. Pusztai,[1] and P. Helander[2]
[1]*Department of Radio and Space Science, Chalmers University of Technology and Euratom-VR Association, Göteborg, Sweden*
[2]*Max-Planck-Institut für Plasmaphysik, Greifswald, Germany*

(Received 28 January 2008; accepted 22 May 2008; published online 30 July 2008)

The collisionality dependence of the quasilinear particle flux due to the ion temperature gradient (ITG) and trapped electron mode (TEM) instabilities is studied by including electron collisions modeled by a pitch-angle scattering collision operator in the gyrokinetic equation. The inward transport due to ITG modes is caused mainly by magnetic curvature and thermodiffusion and can be reversed as electron collisions are introduced, if the plasma is far from marginal stability. However, if the plasma is close to marginal stability, collisions may even enhance the inward transport. The sign and the magnitude of the transport are sensitive to the form of the collision operator, to the magnetic drift normalized to the real frequency of the mode, and to the density and temperature scale lengths. These analytical results are in agreement with previously published gyrokinetic simulations. Unlike the ITG-driven flux, the TEM-driven flux is expected to be outwards for conditions far from marginal stability and inwards otherwise. © *2008 American Institute of Physics*. [DOI: 10.1063/1.2946433]

I. INTRODUCTION

Density peaking in tokamak plasmas has been shown to decrease with increasing collisionality in ASDEX Upgrade[1] and JET (Joint European Torus)[2] H-modes.[3–5] These experimental results suggest that the particle transport, which is usually dominated by ITG- and TEM-driven turbulence, depends on the collisionality, although it has been suggested that the source from ionization may also play an important role.[6,7]

In the collisionless limit, numerical simulations of ITG-mode driven turbulence give an inward particle flux in fluid, gyrofluid, and gyrokinetic descriptions. The inward flow is caused mainly by magnetic curvature and thermodiffusion. However, nonlinear gyrokinetic calculations show that even a small value of the collisionality affects strongly the magnitude and sign of the anomalous particle flows.[8] The inward particle flow obtained in the collisionless limit is rapidly converted to outward flow as electron-ion collisions are included. Linear gyrokinetic calculations with GS2 and a quasilinear model for the particle fluxes[9] have confirmed the strong collisionality dependence of the quasilinear particle flux for small collisionalities and show a good agreement with nonlinear gyrokinetic results from Ref. 8. Both gyrokinetic models find that the total particle flux becomes directed outward for much smaller values of collisionality than the lowest collisionality presently achieved in tokamaks. This means that according to these simulations, for present tokamak experiments the particle flow should be outward.

The present paper addresses the collisionality dependence of the quasilinear flux due to ITG and TEM modes. The aim is to derive analytical expressions for the quasilinear flux to show explicitly the dependence on collisionality, density, and temperature gradients, so that the sign and magnitude of the flux can easily be estimated. We focus on the collisionality dependence of the direction and the magnitude of the quasilinear flux, and give approximate analytical expressions for weakly collisional plasmas with large aspect ratio and circular cross section.

The collisionality dependence has previously been studied in Refs. 10 and 11 by approximating the collision operator with an energy-dependent Krook operator. The main difference between this paper and the references above is the form of the collision operator. Here we use a pitch-angle scattering collision operator, but we include the results for the Krook operator for comparison and completeness. As we will show here, the form of the collision operator determines the scaling with collisionality and therefore affects the collisionality threshold at which the particle flow reverses. The eigenfrequency and growth rate of the modes are only weakly dependent on the collisionality,[8] and in this paper we do not analyze the dispersion relation and the stability boundaries, but instead focus on the quasilinear particle flux driven by the mode. The collisionality dependence of the quasilinear flux due to the TEM instability has been studied in Ref. 12 using a pitch-angle scattering collision operator, and here we generalize the expression presented there by including the magnetic drift.

The structure of the paper is the following: In Sec. II the general gyrokinetic formalism is presented. In Sec. III approximate solutions of the gyrokinetic equation are given in the limit of high mode numbers and the perturbed electron density is calculated. In Sec. IV the quasilinear flux is calculated and the effect of collisions is discussed. The possibility of flux reversal, comparison with previous work and the validity of our approximations are discussed in Sec. V. Finally, the results are summarized in Sec. VI.

II. GYROKINETIC EQUATION

We consider an axisymmetric, large aspect ratio torus with circular magnetic surfaces. The nonadiabatic part of the perturbed distribution function is given by the linearized gyrokinetic equation[10]

$$\frac{v_\parallel}{qR}\frac{\partial g_a}{\partial \theta} - i(\omega - \omega_{Da})g_a - C_a(g_a) = -i\frac{e_a f_{a0}}{T_a}(\omega - \omega_{*a}^T)\phi J_0(z_a), \tag{1}$$

where θ is the extended poloidal angle, ϕ is the perturbed electrostatic potential, $f_{a0}=n_a(m_a/2\pi T_a)^{3/2}\exp(-w/T_a)$ is the equilibrium Maxwellian distribution function, $w=m_a v^2/2$, n_a, T_a, and e_a are the density, temperature, and charge of species a, respectively, $\omega_{*a}=-k_\theta T_a/e_a B L_{na}$ is the diamagnetic frequency, $\omega_{*a}^T=\omega_{*a}[1+(w/T_a-3/2)\eta_a]$, $\eta_a=L_{na}/L_{Ta}$, $L_{na}=-[\partial(\ln n_a)/\partial r]^{-1}$, $L_{Ta}=-[\partial(\ln T_a)/\partial r]^{-1}$, are the density and temperature scale lengths, respectively, k_θ is the poloidal wave-number, $\omega_{Da}=-k_\theta(v_\perp^2/2+v_\parallel^2)(\cos\theta+s\theta\sin\theta)/\omega_{ca}R$ is the magnetic drift frequency, $\omega_{ca}=e_aB/m_a$ is the cyclotron frequency, q is the safety factor, $s=(r/q)(dq/dr)$ is the magnetic shear, r is the minor radius, R is the major radius, J_0 is the Bessel function of order zero, and $z_a=k_\perp v_\perp/\omega_{ca}$.

III. PERTURBED ELECTRON DENSITY RESPONSE

Turning to the electron kinetic equation, we retain collisions and use a pitch-angle scattering operator

$$C_e = \nu_e(v)\frac{2\xi}{B}\frac{\partial}{\partial\lambda}\xi\lambda\frac{\partial}{\partial\lambda} \equiv \nu_e(v)\mathcal{L}, \tag{2}$$

where $\nu_e(v)=\nu_T/x^3$, $x=v/v_{Te}$, $\xi=v_\parallel/v$, and $\lambda=\mu/w$ with $\mu=m_a v_\perp^2/2B$. If the electron distribution is expanded as $g_e=g_{e0}+g_{e1}+\cdots$ in the smallness of the normalized collisionality $\nu_{*e}=\nu_e/\epsilon\omega_b\ll 1$ and $\omega/\omega_b\ll 1$, where ω_b is the bounce frequency, then in lowest order we have $\partial g_{e0}/\partial\theta=0$. In next order, we arrive at

$$i(\omega-\langle\omega_{De}\rangle)g_{e0} + \langle C_e(g_{e0})\rangle = \frac{ie\langle\phi\rangle}{T_e}(\omega_{*e}^T-\omega)f_{e0}, \tag{3}$$

where $\langle\cdots\rangle$ is the orbit average. The circulating electrons are assumed to be adiabatic, while in the trapped region g_{e0} is given by

$$(\omega-\langle\omega_{De}\rangle)g_{e0} - \frac{2i\nu_e\sqrt{2\epsilon}}{\hat{\tau}_B B}\frac{\partial}{\partial\lambda}\lambda\left(\int \xi d\theta\right)\frac{\partial g_{e0}}{\partial\lambda} = -\frac{e\langle\phi\rangle}{T_e}(\omega-\omega_{*e}^T)f_{e0}, \tag{4}$$

where the orbit-averaged precession frequency for trapped electrons is

$$\langle\omega_{De}\rangle = \omega_{D0}\left[\frac{E(\kappa)}{K(\kappa)} - \frac{1}{2} + \frac{2rq'}{q}\left(\frac{E(\kappa)}{K(\kappa)}+\kappa-1\right)\right], \tag{5}$$

where $\omega_{D0}=-k_\theta v^2/\omega_{ce}R$ and E, K are the complete elliptic functions with the argument $\kappa=(1-\lambda B_0(1-\epsilon))/2\epsilon\lambda B_0$, where B_0 is the flux-surface averaged magnetic field and $\epsilon=r/R$. Performing the orbit average on the scattering operator, Eq. (4) becomes

$$(\omega-\langle\omega_{De}\rangle)g_{e0} - \frac{i\nu_e}{\epsilon\hat{\tau}_B}\frac{\partial}{\partial\kappa}\hat{J}(\kappa)\frac{\partial g_{e0}}{\partial\kappa} = -\frac{e\langle\phi\rangle}{T_e}(\omega-\omega_{*e}^T)f_{e0}, \tag{6}$$

where $\hat{J}=E(\kappa)+(\kappa-1)K(\kappa)$ and $\hat{\tau}_B=K(\kappa)$. We introduce a parameter $\hat{\nu}\equiv\nu_e/\omega_0\epsilon$, where $\omega_0=\omega/y$, $y=\sigma+i\hat{\gamma}$, $\sigma=\mathrm{sign}(\mathrm{Re}\{\omega\})$ denotes the sign of the real part of the eigenfrequency, and $\hat{\gamma}=\gamma/\omega_0$ is the normalized growth rate. The equation for g_{e0} is

$$\hat{\nu}(g_{e0}'' + (\ln\hat{J})'g_{e0}') + i\frac{K}{\hat{J}}\left(y - \frac{\langle\omega_{De}\rangle}{\omega_0}\right)g_{e0} = i\frac{SK}{\omega_0\hat{J}}, \tag{7}$$

where $S=-(e\langle\phi\rangle/T_e)(\omega-\omega_{*e}^T)f_{e0}$. The perturbed electrostatic potential is approximated by $\phi(\theta)=\phi_0(1+\cos\theta)/2[H(\theta+\pi)-H(\theta-\pi)]$, where H is the Heaviside function and then $\langle\phi\rangle=\phi_0E(\kappa)/K(\kappa)$. Assuming weakly collisional plasmas such that $\hat{\nu}\ll 1$, the WKB solution to the homogeneous equation $\hat{\nu}(g_{e0}''+(\ln\hat{J})'g_{e0}')=\Omega^2 g_{e0}$, where $\Omega^2=-i(y-\langle\omega_{De}\rangle/\omega_0)K/\hat{J}$, is

$$g_{\mathrm{hom}}(\kappa) = \frac{1}{\sqrt{\Omega\hat{J}}}\left[c_1\sinh\left(\hat{\nu}^{-1/2}\int^\kappa\Omega(z)dz\right) + c_2\cosh\left(\hat{\nu}^{-1/2}\int^\kappa\Omega(z)dz\right)\right]. \tag{8}$$

The solution of the inhomogeneous equation can then be obtained with the method of variation of parameters, using the boundary conditions at $\kappa=0$ and $\kappa=1$ to determine the integration constants c_1 and c_2.

To make further progress analytically, we need to approximate the elliptic functions with their asymptotic limits for small argument, as was done in Ref. 12, so that $K(\kappa)/\hat{J}(\kappa)=2/\kappa$. The homogeneous solution becomes

$$g_{\mathrm{hom}}(\kappa) = \frac{1}{(\kappa u)^{1/4}}[c_1\sinh(2\sqrt{\kappa u/\hat{\nu}}) + c_2\cosh(2\sqrt{\kappa u/\hat{\nu}})], \tag{9}$$

where $u=-i(2y-\hat{\omega}_D)$, and $\hat{\omega}_D=\omega_{D0}/\omega_0$ is the normalized magnetic drift frequency. The inhomogeneous part of the distribution is given by

$$g_{\mathrm{inhom}}(\kappa) = \frac{-2i\hat{S}}{u\omega_0}\left[1 - \frac{\sqrt{\pi}}{4z}[e^{z^2}\mathrm{Erf}(z) + e^{-z^2}\mathrm{Erfi}(z)]\right], \tag{10}$$

where $z=\sqrt{2}(\kappa u/\hat{\nu})^{1/4}$, $\hat{S}=SK(\kappa)/E(\kappa)$, $\mathrm{Erf}(z)$ is the error function, and $\mathrm{Erfi}(z)=\mathrm{Erf}(iz)/i$ is the imaginary error function. In the limit of $z\to\infty$ (consistent with the assumption $\hat{\nu}\ll 1$), the error functions can be expanded, and the inhomogeneous solution simplifies to

$$g_{\mathrm{inhom}}(\kappa)=\frac{-i\hat{S}}{2u\omega_0}(4-\sqrt{\pi}e^{z^2}/z). \tag{11}$$

Since $g_{e0}(\kappa=0)$ is regular, we choose $c_2=0$, and the boundary condition $g_{e0}(\kappa=1)=0$ (Ref. 12) gives $c_1=-g_{\mathrm{inhom}}(1)u^{1/4}/\sinh(2\sqrt{u/\hat{\nu}})$, so that the solution for the perturbed trapped-electron distribution is

$$g_{e0}=\frac{-i\hat{S}(4-\sqrt{\pi}e^{z^2}/z)}{2u\omega_0}+\frac{i\hat{S}(4-\sqrt{\pi}e^{z^2/\sqrt{\kappa}}\kappa^{1/4}/z)}{2u\kappa^{1/4}\omega_0}\frac{\sinh(z^2)}{\sinh(z^2/\sqrt{\kappa})}, \tag{12}$$

except in a narrow boundary layer close to $\kappa=0$, that has a negligible contribution to the velocity space integrals. The nonadiabatic part of the perturbed trapped-electron density is proportional to

$$\left\langle\int g_{e0}d^3v\right\rangle=4\sqrt{2\epsilon}\int_0^\infty v^2dv\int_0^1 K(\kappa)g_{e0}d\kappa=4\sqrt{2\epsilon}\int_0^\infty v^2dvI_1. \tag{13}$$

Using Eq. (12), the integral I_1 becomes

$$I_1=\int_0^1 K(\kappa)g_{e0}d\kappa=-\frac{\pi i\hat{S}}{u^2\omega_0}(u-\sqrt{u\hat{\nu}}), \tag{14}$$

where we retained terms only to the lowest order in $\hat{\nu}^{1/2}$ and we approximated $K(\kappa)\simeq\pi/2$.

The above analysis is not valid in the boundary layer at $\kappa\simeq 1$. The effect of the boundary layer reduces the collisional term, with a factor $\pi/2\sqrt{\ln\hat{\nu}^{-1/2}}$ (see Appendix A for details). The reduction is less than 20% in the experimentally relevant collisionality regime, and in the following analysis this will be neglected.

Expanding in the limit of small $\hat{\omega}_D$ and keeping terms to the first order, we have

$$\frac{2I_1}{\pi}=\frac{\hat{S}(8y^2-3i\sqrt{2}\hat{\omega}_D\sqrt{-iy\hat{\nu}}+4y(\hat{\omega}_D-i\sqrt{-2iy\hat{\nu}}))}{8y^3\omega_0}. \tag{15}$$

Introducing $\hat{\omega}_{Dt}=\hat{\omega}_D/x^2$, $\hat{\omega}_{*e}=\omega_{*e}/\omega_0$ and $\hat{\nu}_t=\hat{\nu}x^3$, we obtain

$$\left\langle\int g_{e0}d^3v\right\rangle=\frac{\pi^{3/2}S_0}{8}\left\{\left(1-\frac{\hat{\omega}_{*e}}{y}\right)+\frac{3\hat{\omega}_{Dt}}{4y}\left(1-(1+\eta_e)\frac{\hat{\omega}_{*e}}{y}\right)\right\}-i\frac{\pi\Gamma(3/4)S_0\sqrt{-i2y\hat{\nu}_t}}{8y}\left\{1+(3\eta_e-4)\frac{\hat{\omega}_{*e}}{4y}+\frac{9\hat{\omega}_{Dt}}{64y}\times\left(4-(4+\eta_e)\frac{\hat{\omega}_{*e}}{y}\right)\right\}, \tag{16}$$

where $S_0=-(e\phi_0/T_e)n_e4\sqrt{2\epsilon}/\pi^{3/2}$. Neglecting the nonadiabatic circulating electron response, the perturbed electron density is

$$\frac{\hat{n}_e}{n_e}=\frac{e\phi_0}{2T_e}\left\{1-\sqrt{2\epsilon}\left[\left(1-\frac{\hat{\omega}_{*e}}{y}\right)+\frac{3\hat{\omega}_{Dt}}{4y}\times\left(1-(1+\eta_e)\frac{\hat{\omega}_{*e}}{y}\right)\right]+\frac{\Gamma(3/4)i\sqrt{-iy\epsilon\hat{\nu}_t}}{\sqrt{\pi}y}\times\left[1+(3\eta_e-4)\frac{\hat{\omega}_{*e}}{4y}+\frac{9\hat{\omega}_{Dt}}{64y}\times\left(4-(4+\eta_e)\frac{\hat{\omega}_{*e}}{y}\right)\right]\right\}. \tag{17}$$

IV. QUASILINEAR PARTICLE FLUX

The quasilinear particle flux is given by[13]

$$\Gamma_e=\mathrm{Re}(\hat{n}_e v_E^*)=\frac{k_\theta\rho_e}{2eB}\left|\frac{e\phi_0}{T_e}\right|^2\mathrm{Im}\left(\frac{\hat{n}_e/n_e}{e\phi_0/T_e}\right), \tag{18}$$

where the radial $\boldsymbol{E}\times\boldsymbol{B}$ velocity is $v_E\approx -ik_\theta\phi_0/2B$. Taking the imaginary part of the perturbed electron density from Eq. (17), we obtain

$$\mathrm{Im}\left(\frac{\hat{n}_e/n_e}{e\phi_0/T_e}\right)=-\sqrt{\frac{\epsilon}{2}}\mathrm{Im}\left\{-\frac{\hat{\omega}_{*e}}{y}+\frac{3\hat{\omega}_{Dt}}{4y}\left[1-(1+\eta_e)\frac{\hat{\omega}_{*e}}{y}\right]\right\}+\frac{\Gamma(3/4)\sqrt{\epsilon\hat{\nu}_t}}{\sqrt{\pi}}\mathrm{Im}\left\{\frac{i\sqrt{-iy}}{y}\left[1+\left(\frac{3}{4}\eta_e-1\right)\frac{\hat{\omega}_{*e}}{y}+\frac{9\hat{\omega}_{Dt}}{16y}\left(1-\left(1+\frac{\eta_e}{4}\right)\frac{\hat{\omega}_{*e}}{y}\right)\right]\right\}. \tag{19}$$

The imaginary part of the perturbed density is sensitive to the sign of the real part of the eigenfrequency σ, and the magnitude of the normalized growth rate $\hat{\gamma}$. In the following analysis the quasilinear flux will be calculated for negative (ITG) and positive (TEM) signs.

A. ITG

ITG modes propagate in the ion diamagnetic direction, so the real part of the eigenfrequency is negative. Figure 1 shows the quasilinear electron flux from Eqs. (18) and (19) normalized to $p_e k_\theta/(2eB)|e\phi_0/T_e|^2\sqrt{\epsilon}$ as function of normalized collisionality for various values of $\hat{\omega}_{Dt}$ and η_e for a case where the plasma is far from marginal stability: $\hat{\gamma}=0.7$.

In the absence of collisions, the flux is inwards if the curvature and thermodiffusive fluxes (the terms proportional to $\hat{\omega}_{Dt}$ and η_e in the first row of Eq. (19)) dominate over diffusion. If collisions are included, the particle flux may be reversed, if the part of the flux that is dependent on the collisionality is positive. This reversal happens, for instance, for $\hat{\omega}_{Dt}=0.2$ and $\eta_e=4.5$ [see Fig. 1(d)].

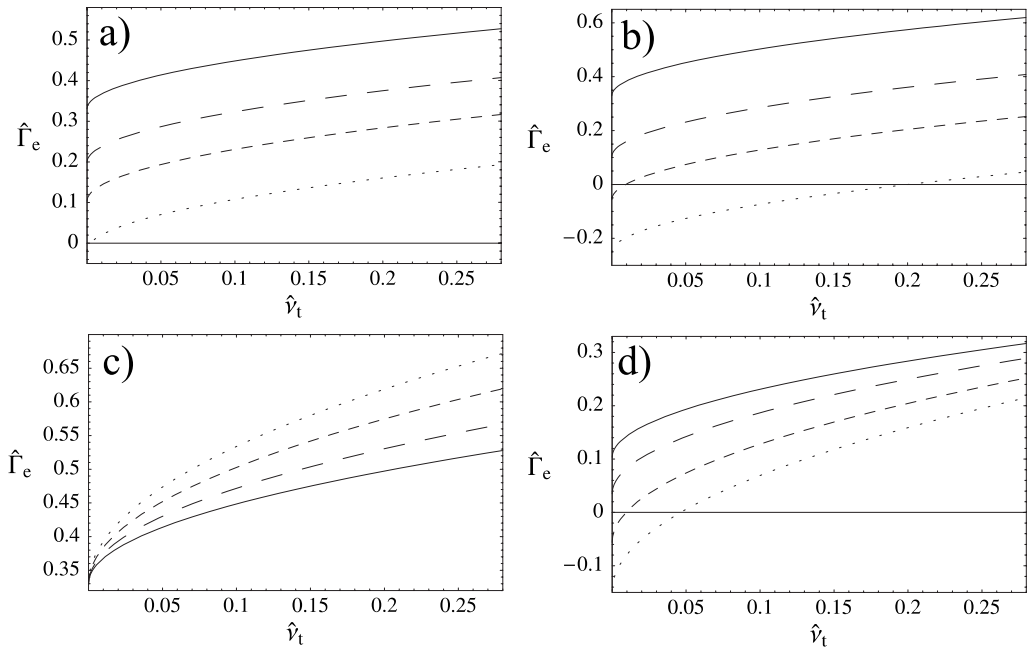

FIG. 1. Normalized quasilinear electron flux driven by ITG as function of normalized collisionality for $\hat{\gamma}=0.7$ and $\hat{\omega}_{*e}=1$. In the upper figures (a and b): from above $\hat{\omega}_{Dt}$ is 0 (solid), 0.1 (long-dashed), 0.2 (short-dashed), and 0.4 (dotted). (a) $\eta_e=3$ and (b) $\eta_e=6.5$. In the lower figures: η_e is 3 (solid), 4.5 (long-dashed), 6.5 (short-dashed), and 8.5 (dotted). (c) $\hat{\omega}_{Dt}=0$ and (d) $\hat{\omega}_{Dt}=0.2$.

However, if the ITG-instability growth rate is weak ($\hat{\gamma} \ll 1$) and η_e is large, the situation is completely different. Figure 2 shows the normalized quasilinear electron flux for the same parameters as in Fig. 1, but for $\hat{\gamma}=0.1$, representing a case close to marginal stability. The term proportional to the $\sqrt{\hat{\nu}_t}$ will change sign and now this will also lead to an inward flux. If the magnetic drift is high enough to give an inward flux for zero collisionality, then collisions will enhance this and the flux will therefore never be reversed. If the magnetic drift is very small, the flux is outwards for $\hat{\nu}_t=0$. Then collisions may reverse the sign of the flux, but now from outwards to inwards.

It is instructive to expand Eq. (19) for small $\hat{\gamma}$, and show explicitly the sign of the different terms in the expression for the flux. If $y=\omega/\omega_0=-1+i\hat{\gamma}$, then to lowest order in $\hat{\gamma}$, we have

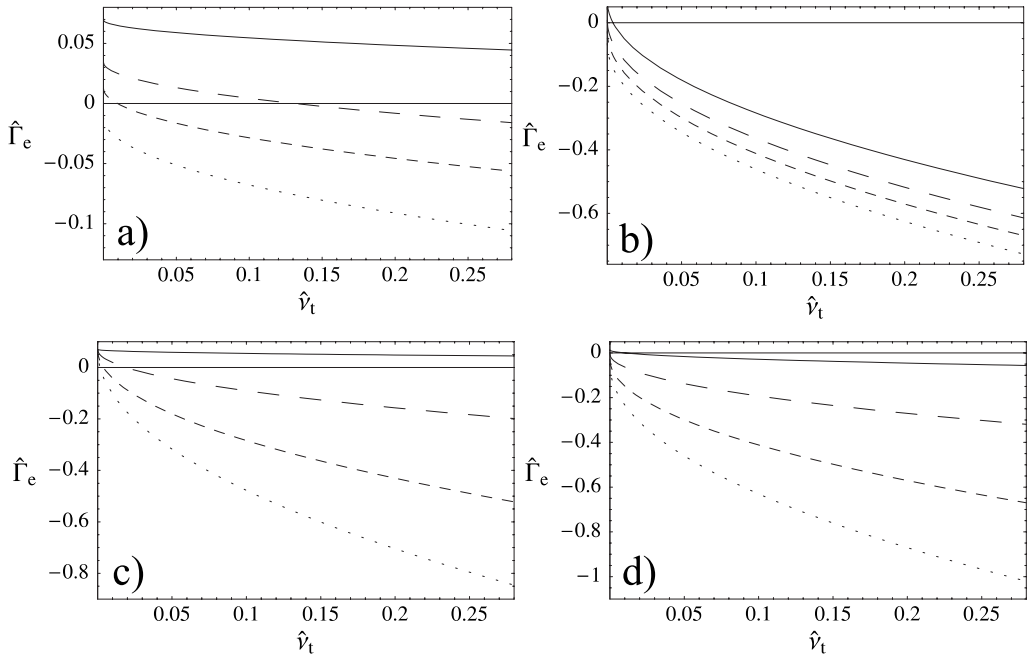

FIG. 2. Same as Fig. 1, but for $\hat{\gamma}=0.1$.

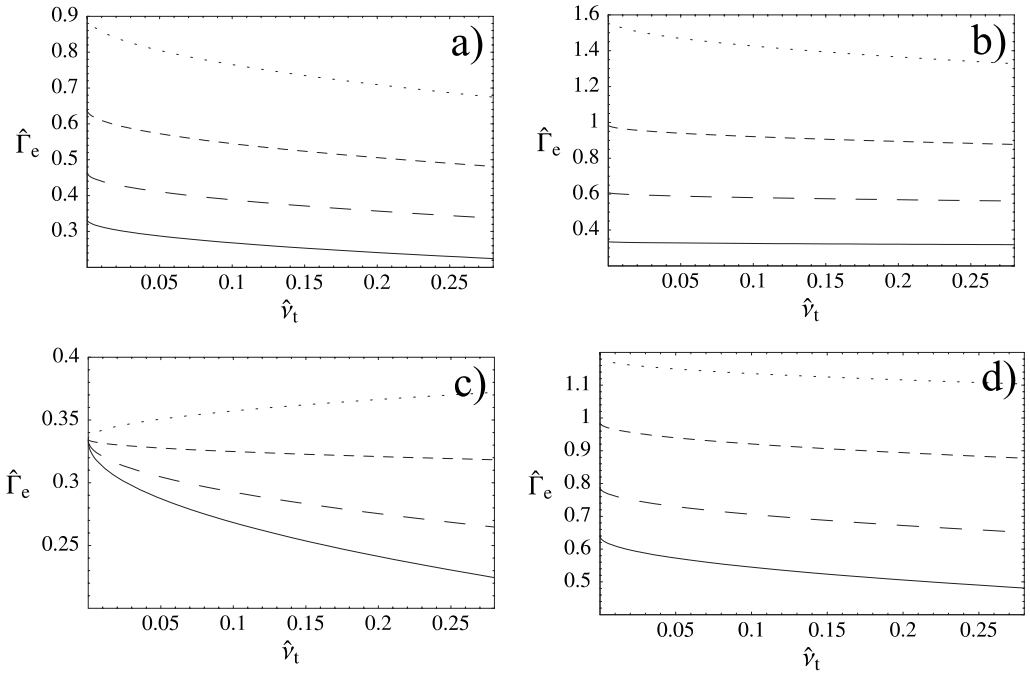

FIG. 3. Normalized quasilinear electron flux driven by TEM as function of normalized collisionality for $\hat{\gamma}=0.7$ and $\hat{\omega}_{*e}=1$. In the upper figures: from below $\hat{\omega}_{Dt}$ is 0 (solid), 0.2 (long-dashed), 0.4 (short-dashed), and 0.6 (dotted). (a) $\eta_e=3$ and (b) $\eta_e=8.5$. In the lower figures: from below η_e is 3 (solid), 4.5 (long-dashed), 6.5 (short-dashed), and 8.5 (dotted). (c) $\hat{\omega}_{Dt}=0$ and (d) $\hat{\omega}_{Dt}=0.2$.

$$\Gamma_e^{\mathrm{ITG}} = \frac{k_\theta p_e}{2eB}\left|\frac{e\phi_0}{T_e}\right|^2\left\{\sqrt{\frac{\epsilon}{2}}\left[1-\frac{3\hat{\omega}_{Dt}}{2}(1+\eta_e)\right]\hat{\gamma}\hat{\omega}_{*e} - \sqrt{\frac{\epsilon}{2}}\frac{3\hat{\omega}_{Dt}\hat{\gamma}}{4} - \frac{\Gamma(3/4)\sqrt{\epsilon\hat{\nu}_t}}{\sqrt{2\pi}}\left\{-1+\frac{\hat{\gamma}}{2}+\left(\frac{3}{4}\eta_e-1\right)\right.\right.$$
$$\times\left(1-\frac{3\hat{\gamma}}{2}\right)\hat{\omega}_{*e}+\frac{9\hat{\omega}_{Dt}}{16}\left[1-\frac{3\hat{\gamma}}{2}+\left(1+\frac{\eta_e}{4}\right)\right.$$
$$\left.\left.\left.\times\left(1-\frac{5\hat{\gamma}}{2}\right)\hat{\omega}_{*e}\right]\right\}\right\}. \tag{20}$$

If the plasma is close to marginal instability ($\hat{\gamma}\simeq 0$), collisions (represented by the term proportional to $\sqrt{\hat{\nu}_t}$) lead to an inward flux if $\eta_e > \eta_{\mathrm{crit}}$:

$$\eta_{\mathrm{crit}} = \frac{4[16(1+\hat{\omega}_{*e})-9\hat{\omega}_{Dt}(1+\hat{\omega}_{*e})]}{3(16+3\hat{\omega}_{Dt})\hat{\omega}_{*e}}. \tag{21}$$

For typical experimental parameters, η_e is expected to be larger than η_{crit}, and therefore the total flux is expected to be inwards. However, if the plasma is further away from marginal instability, so that $\hat{\gamma}>2/3$, the terms to $1-3\hat{\gamma}/2$ and $1-5\hat{\gamma}/2$ change sign, and then collisions will lead to an outward flux, as Fig. 1 shows. Note that the figures show the quasilinear flux calculated from the unexpanded solution (Eqs. (14) and (18)) and they are valid even for $\hat{\gamma}\simeq 1$.

B. TEM

The real part of the eigenfrequency is positive, and this means that $y=\omega/\omega_0=1+i\hat{\gamma}$ and the electron flux to lowest order is

$$\Gamma_e^{\mathrm{TEM}} = \frac{k_\theta p_e}{2eB}\left|\frac{e\phi_0}{T_e}\right|^2\left\{\sqrt{\frac{\epsilon}{2}}\left[1+\frac{3\hat{\omega}_{Dt}}{2}(1+\eta_e)\right]\hat{\gamma}\hat{\omega}_{*e} - \sqrt{\frac{\epsilon}{2}}\frac{3\hat{\omega}_{Dt}\hat{\gamma}}{4} - \frac{\Gamma(3/4)\sqrt{\epsilon\hat{\nu}_t}}{\sqrt{2\pi}}\left\{1-\frac{\hat{\gamma}}{2}+\left(\frac{3}{4}\eta_e-1\right)\right.\right.$$
$$\times\left(1-\frac{3\hat{\gamma}}{2}\right)\hat{\omega}_{*e}+\frac{9\hat{\omega}_{Dt}}{16}\left[1-\left(1+\frac{\eta_e}{4}\right)\right.$$
$$\left.\left.\left.\times\left(1-\frac{5\hat{\gamma}}{2}\right)\hat{\omega}_{*e}\right]\right\}\right\}. \tag{22}$$

There are two main differences compared with the ITG-driven flux. First, the part of the flux that is driven by the curvature has opposite sign compared with ITG, and therefore contributes to the outward flux instead of driving an inward pinch. Second, the part of the flux that arises due to collisions is different and may have opposite sign compared with the ITG case, depending on the parameters. Figure 3 shows the normalized quasilinear flux for different parameters if the plasma is far from marginal stability ($\hat{\gamma}=0.7$) and Fig. 4 shows the same for $\hat{\gamma}=0.1$. Also here, the magnitude of $\hat{\gamma}$ changes the sign of the flux from outward to inward, and collisions contribute to the inward flux.

C. Collisions modeled by a Krook operator

Starting from the gyrokinetic equation for the electrons but modeling the collision operator with an energy-dependent Krook operator, we have

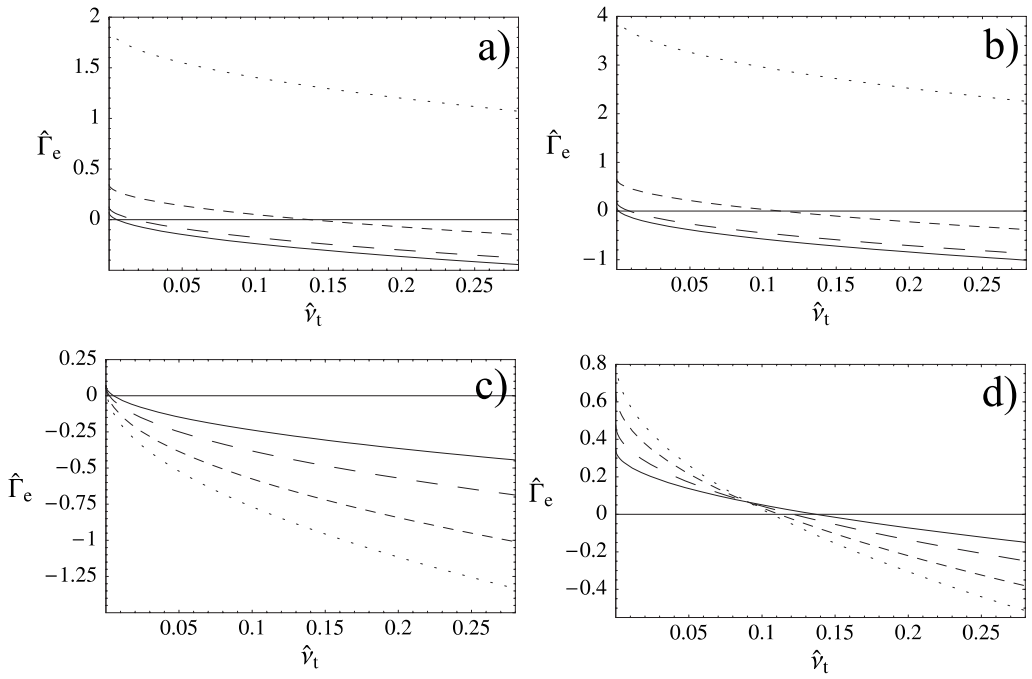

FIG. 4. Same as in Fig. 3, but for $\hat{\gamma}=0.1$.

$$i(\omega-\langle\omega_{De}\rangle)g_{e0}-\nu_{\rm eff}g_{e0}=-\frac{e\phi_0}{T_e}(\omega-\omega_{*e}^T)f_{e0} \tag{23}$$

so that

$$g_{e0}=-\frac{e\phi_0}{T_e}\frac{\omega-\omega_{*e}^T}{\omega-\langle\omega_{De}\rangle+i\nu_{\rm eff}}f_{e0}, \tag{24}$$

where $\nu_{\rm eff}=\nu_T/\epsilon x^3$.

The velocity-space integral of the perturbed electron distribution can be used to determine the imaginary part of the perturbed electron density, and that gives the quasilinear flux from Eq. (18). If the plasma is far from marginal stability, the results for the pitch-angle scattering and Krook operator are qualitatively same, as shown in the upper figures of Fig. 5. However, as the lower figures in Fig. 5 show, as we approach marginal stability, the form of the collision operator matters more and more, and both the sign and the magnitude of the flux may be very different.

V. DISCUSSION

We have shown that in plasmas that are dominated by ITG turbulence and are far from marginal stability the sign of the electron flux will be changed from inward to outward if the collisionality is increased. Figure 6 shows the threshold in collisionality for which the flux reverses, i.e., $\hat{\nu}_c$, as a function of η_e for different values of the normalized magnetic drift frequency. The red curves correspond to the pitch-angle scattering model-operator and the black curves correspond to the Krook model. It is interesting to see that the pitch-angle scattering operator gives lower threshold for flux reversal. If we compare the collisionality for zero flux in Fig. 4 in Ref. 8, we find that our result is of the same order of magnitude. Figure 4 in Ref. 8 is computed for $\eta_e=3$, $R=3$ m, $r=0.5$ m, $a=1$ m, $s=1$, $q=2$. For these parameters the trapped-electron flow changes sign for $\nu_e\simeq 0.006c_s/a$, where $c_s=\sqrt{T_e/m_i}$ is the ion sound speed. This collisionality corresponds to $\hat{\nu}_c\simeq 0.1$. This is in agreement with our threshold, shown in Fig. 6 for $\eta_e=3$ and $\hat{\omega}_{Dt}=0.7$. Note that Fig. 4 in Ref. 8 is the result of a *nonlinear* gyrokinetic simulation so $\hat{\omega}_{Dt}$ is not constant and therefore exact comparison is not possible.

The analytical calculation presented in this paper is an attempt to shed light on the numerical calculations mentioned above. For this purpose it is necessary to make a number of simplifications, some of which may be justified within a rigorous ordering scheme. However, it should be noted that some approximations are more qualitative, in particular those having to do with the mode structure, which we do not solve for. The approximation we use for the perturbed electrostatic potential breaks down for low shear or near marginal instability. It appears that the qualitative features of the transport are captured by our calculations, but for quantitatively accurate results one of course has to resort to numerical simulations.

As we have seen, the effect of magnetic drift is important to understand the sign change of the quasilinear flux due to the ITG modes. The magnetic drift gives an inward flux for zero collisionality, but this is reversed when $\hat{\nu}_t>\hat{\nu}_c$.

VI. CONCLUSIONS

The collisionality dependence of the quasilinear particle flux due to microinstabilities has been determined for large aspect ratio, circular cross section plasmas. It has been shown that if the plasma is far from marginal stability, the

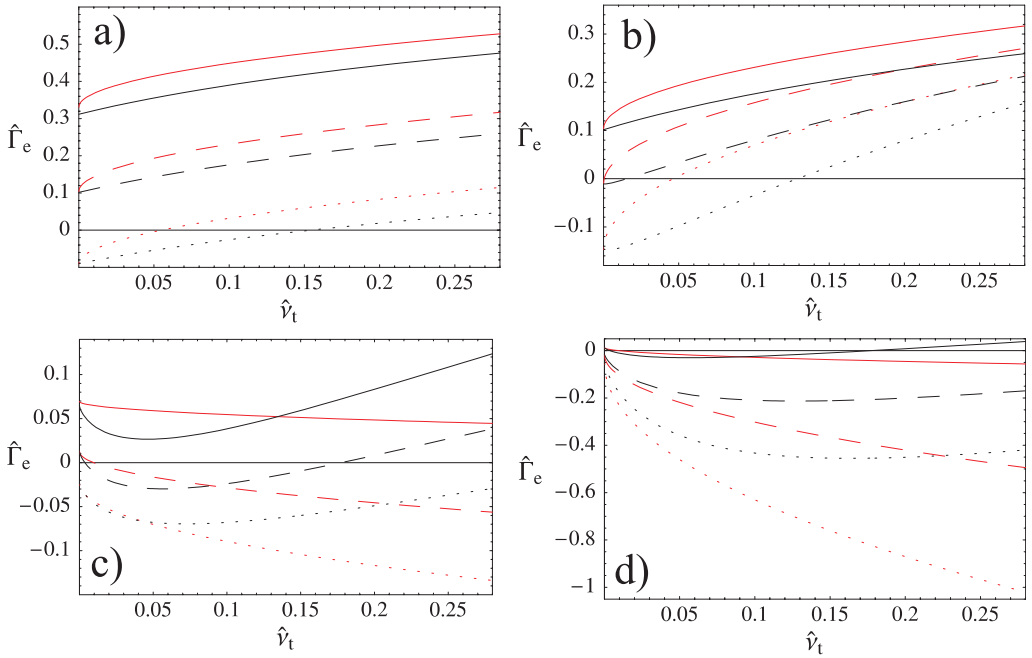

FIG. 5. (Color) Normalized quasilinear electron flux driven by ITG as function of normalized collisionality for $\hat{\omega}_{*e}=1$. The red curves are for the pitch-angle scattering operator and the black are for the Krook operator. In the left figures (a and c) $\eta_e=3$ and from above: $\hat{\omega}_{Dt}$ is 0 (solid), 0.2 (dashed), and 0.6 (dotted). On the right, figures (b and d) $\hat{\omega}_{Dt}=0.2$ and from above: η_e is 3 (solid), 5.5 (dashed), and 8.5 (dotted). The upper figures (a and b) are for $\hat{\gamma}=0.7$, and the lower (c and d) for $\hat{\gamma}=0.1$.

inward transport due to ITG modes is reversed as electron collisions are introduced, in agreement with nonlinear gyrokinetic simulations. However, if the plasma is close to marginal stability, collisions will lead to an additional inward flux, and therefore the total flux is expected to be inwards. The transport is therefore affected significantly by the parameter η_e, both directly via the terms proportional to η_e in the expression for the flux, but also indirectly via the ITG growth rate, which is important to determine the sign of the flux.

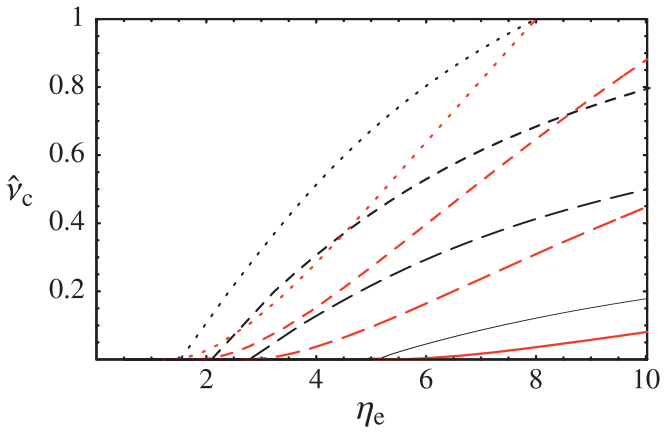

FIG. 6. (Color) Collisionality threshold as a function of η_e for $\hat{\gamma}=0.7$ and $\hat{\omega}_{*e}=1$. Above the lines, the transport is outwards, and below it is inwards. The different lines correspond different values of $\hat{\omega}_{Dt}$: from below $\hat{\omega}_{Dt}$ is 0.2 (solid), 0.4 (long-dashed), 0.6 (short-dashed), and 0.8 (dotted). The red lines are for the pitch-angle scattering operator and the black are for the Krook operator.

If the electron collisions are modeled with a pitch-angle scattering collision operator, the particle flux is proportional to the square-root of the collisionality. The choice of the model collision operator affects the collisionality threshold for the reversal of the particle flux; i.e., $\hat{\nu}_c$. This is especially important when the plasma is close to marginal stability. The collisionality threshold $\hat{\nu}_c$ depends on the magnitude of the normalized magnetic drift $\hat{\omega}_{Dt}$ and the ratio of density and temperature scale lengths; i.e., η_e. For higher η_e and higher $\hat{\omega}_{Dt}$, higher collisionality is needed to reverse the particle flux.

The magnitude and the sign of the TEM-driven quasilinear flux has also been determined. The TEM-driven flux is expected to be outwards if the plasma is far from marginal stability and inwards otherwise, for typical experimental parameters, and the presence of collisions contributes to the inward flow.

ACKNOWLEDGMENTS

This work was funded by the European Communities under Association Contract between EURATOM, Germany and *Vetenskapsrådet*. The authors would like to thank Dr. J. Hastie and Dr. P. Catto for useful discussions of the paper. The views and opinions expressed herein do not necessarily reflect those of the European Commission.

APPENDIX A: BOUNDARY LAYER ANALYSIS FOR $\kappa \simeq 1$

In the outer region, far away from the trapped/passing boundary we can neglect collisions, and the solution of Eq. (7) is

$$g_{\text{outer}} = \frac{\hat{S}E(\kappa)}{(\omega - \langle\omega_{De}\rangle)K(\kappa)}. \tag{A1}$$

The width of the boundary layer can be estimated by comparing $|\hat{\nu} g''_{e0}|$ using the outer solution for g_{e0} and the term on the right-hand-side of Eq. (7), leading to $(1-\kappa) \sim \hat{\nu}^{1/2}$.

In the inner region we can approximate the elliptical integrals with their asymptotic forms for $\kappa = 1$, giving $E(\kappa) \simeq 1$, $\hat{J}(\kappa) \simeq 1$, $K(\kappa) \simeq \ln(1/\sqrt{1-\kappa}) \simeq \ln \hat{\nu}^{-1/4} \equiv \hat{K}$. Changing variables in Eq. (7) to $t = (1-\kappa)/\sqrt{\hat{\nu}}$ gives

$$\frac{\partial^2 g_{\text{inner}}}{\partial t^2} + i\hat{K}\left(y - \frac{\langle\omega_{De}\rangle}{\omega_0}\right) g_{\text{inner}} = i\frac{\hat{S}}{\omega_0}, \tag{A2}$$

and the solution is

$$g_{\text{inner}} = \frac{\hat{S}}{(\omega - \langle\omega_{De}\rangle)\hat{K}} + \hat{c}_1 \exp[-(1-\kappa)\sqrt{\hat{u}\hat{K}/\hat{\nu}}] + \hat{c}_2 \exp[(1-\kappa)\sqrt{\hat{u}\hat{K}/\hat{\nu}}], \tag{A3}$$

where $\hat{u} = -i(y - \langle\omega_{De}\rangle/\omega_0)$. $\hat{c}_1$ is determined by the boundary condition $g_{e0}(\kappa = 1) = 0$ and $\hat{c}_2 = 0$ to match the inner and outer solutions. The global solution is then

$$g_{e0} = \frac{\hat{S}E}{(\omega - \langle\omega_{De}\rangle)K}\left\{1 - \exp[-(1-\kappa)\sqrt{\hat{u}\hat{K}/\hat{\nu}}]\right\}. \tag{A4}$$

Using the global solution from Eq. (A4), the collisional term becomes

$$\int_0^1 K(\kappa) \frac{-\hat{S}E(\kappa)}{(\omega - \langle\omega_{De}\rangle)K(\kappa)} \exp[-(1-\kappa)\sqrt{\hat{u}\hat{K}/\hat{\nu}}] d\kappa \simeq -\frac{\hat{S}\sqrt{\hat{\nu}}}{(\omega - \omega_{D0}/2)\sqrt{\hat{u}\hat{K}}} \tag{A5}$$

since the dominant part of the integral comes from $\kappa \simeq 1$. Comparing with the corresponding term in Eq. (14), we find that the effect of the boundary layer reduces the collisional term, with a factor $(\pi/2\sqrt{\ln \hat{\nu}^{-1/2}})$.

APPENDIX B: COMPARISON WITH THE SOLUTION FOR $\hat{\omega}_{Dt} = 0$ IN REF. 12

In Ref. 12, the effect of the magnetic drift has been neglected (that is, $\hat{\omega}_{Dt} = 0$), and the perturbed trapped electron distribution has been calculated to be

$$g_{e0} = -\frac{e\phi_0}{T_e}(1 - \omega^T_{*e}/\omega) f_{e0}\left[1 - \frac{2J_1(a)}{aJ_0(a)}\right], \tag{B1}$$

where $a = (1+i)\sqrt{4\omega\epsilon/\nu_e(v)} \equiv a_r(1+i)$. There is excellent agreement between our results in the limit of $\hat{\omega}_{Dt} = 0$ (both the expanded solution and the full WKB solution) and the one published in Ref. 12. The perturbed electron density is [Eq. (28) of Ref. 12]

$$\frac{\hat{n}_e}{n_e} = \frac{e\phi_0}{T_e}\left\{1 - \frac{8\sqrt{2\epsilon}}{\pi^{3/2}}\int_0^\infty x^2 e^{-x^2} dx\left[1 - \frac{2J_1(a)}{aJ_0(a)}\right] \times \left[1 - \frac{\omega_{*e}}{\omega}[1 - \eta_e(x^2 - 3/2)]\right]\right\}. \tag{B2}$$

If the real part of the frequency is negative ($\omega = -\omega_0 + i\gamma$), where $\omega_0 > 0$, then for $a_r \gg 1$ and $\hat{\gamma} \ll 1$, we have

$$\text{Im}\left(\frac{\hat{n}_e/n_e}{e\phi_0/T_e}\right) = -\frac{2\sqrt{2\epsilon}}{\pi}\left\{\hat{\omega}_{*e}\hat{\gamma} + \Gamma(3/4) \times \sqrt{\frac{\hat{\nu}_t}{\pi}}[1 + \hat{\omega}_{*e}(1 - 3\eta_e/4)]\right\}. \tag{B3}$$

This is in agreement with our results in the limit of $\hat{\omega}_{Dt} = 0$.

[1] S. Günter, C. Angioni, C. Atanasiu, C. Atanasiu, M. Balden, G. Becker, W. Becker, K. Behler, K. Behringer, A. Bergmann, R. Bilato, I. Bizyukov, V. Bobkov, T. Bolzonella, D. Borba, K. Borrass, M. Brambilla, F. Braun, A. Buhler, A. Carlson, A. Chankin, J. Chen, Y. Chen, S. Cirant, G. Conway, D. Coster, T. Dannert, K. Dimova, R. Drube, R. Dux, T. Eich, K. Engelhardt, H.-U. Fahrbach, U. Fantz, L. Fattorini, M. Foley, P. Franzen, J. C. Fuchs, J. Gafert, K. Gal, G. Gantenbein, M. García Muñoz, O. Gehre, A. Geier, L. Giannone, O. Gruber, G. Haas, D. Hartmann, B. Heger, B. Heineman, A. Herrmann, J. Hobirk, H. Hohenöcker, L. Horton, M. Huart, V. Igochine, A. Jacchia, M. Jakobi, F. Jenko, A. Kallenbach, S. Kálvin, O. Kardaun, M. Kaufmann, A. Keller, A. Kendl, M. Kick, J.-W. Kim, K. Kirov, S. Klose, R. Kochergov, G. Kocsis, H. Kollotzek, C. Konz, W. Kraus, K. Krieger, T. Kurki-Suonio, B. Kurzan, K. Lackner, P. T. Lang, P. Lauber, M. Laux, F. Leuterer, L. Likonen, A. Lohs, A. Lorenz, R. Lorenzini, A. Lyssoivan, C. Maggi, H. Maier, K. Mank, A. Manini, M.-E. Manso, P. Mantica, M. Maraschek, P. Martin, K. F. Mast, M. Mayer, P. McCarthy, H. Meyer, D. Meisel, H. Meister, S. Menmuir, F. Meo, P. Merkel, D. Merkl, V. Mertens, F. Monaco, A. Mück, H. W. Müller, M. Münich, H. Murmann, Y.-S. Na, R. Narayanan, G. Neu, R. Neu, J. Neuhauser, D. Nishijima, Y. Nishimura, J.-M. Noterdaeme, I. Nunes, M. Pacco-Düchs, G. Pautasso, A. G. Peeters, G. Pereverzev, S. Pinches, E. Poli, E. Posthumus-Wolfrum, T. Pütterich, R. Pugno, E. Quigley, I. Radivojevic, G. Raupp, M. Reich, R. Riedl, T. Ribeiro, V. Rohde, J. Roth, F. Ryter, S. Saarelma, W. Sandmann, J. Santos, G. Schall, H.-B. Schilling, J. Schirmer, W. Schneider, G. Schramm, J. Schweinzer, S. Schweizer, B. Scott, U. Seidel, F. Serra, C. Sihler, A. Silva, A. Sips, E. Speth, A. Stäbler, K.-H. Steuer, J. Stober, B. Streibl, D. Strintzi, E. Strumberger, W. Suttrop, G. Tardini, C. Tichmann, W. Treutterer, M. Troppmann, M. Tsalas, H. Urano, P. Varela, D. Wagner, F. Wesner, E. Würsching, M. Y. Ye, S.-W. Yoon, Q. Yu, B. Zaniol, D. Zasche, T. Zehetbauer, H.-P. Zehrfeld, M. Ziker, and H. Zohm, Nucl. Fusion **45**, S98 (2005).

[2] P. H. Rebut, Nucl. Fusion **25**, 1011 (1985).

[3] C. Angioni, A. G. Peeters, G. V. Pereverzev, F. Ryter, G. Tardini, and ASDEX Upgrade Team, Phys. Rev. Lett. **90**, 205003 (2003).

[4] C. Angioni, A. G. Peeters, G. V. Pereverzev, F. Ryter, and G. Tardini, Phys. Plasmas **10**, 3225 (2003).

[5] H. Weisen, A. Zabolotsky, C. Angioni, I. Furno, X. Garbet, C. Giroud, H. Leggate, P. Mantica, D. Mazon, J. Weiland, L. Zabeo, K.-D. Zastrow, and JET-EFDA Contributors, Nucl. Fusion **45**, L1 (2005).

[6] M. Valovic, J. Rapp, J. G. Cordey, R. Budny, D. C. McDonald, L. Garzotti, A. Kallenbach, M. A. Mahdavi, J. Ongena, V. Parail, G. Saibene, R. Sartori, M. Stamp, O. Sauter, J. Strachan, W. Suttrop, and the EFDA-JET Workprogramme, Plasma Phys. Controlled Fusion **44**, 1911 (2002).

[7] M. Valovic, R. Budny, L. Garzotti, X. Garbet, A. A. Korotkov, J. Rapp, R. Neu, O. Sauter, P. deVries, B. Alper, M. Beurskens, J. Brzozowski, D. McDonald, H. Leggate, C. Giroud, V. Parail, I. Voitsekhovitch, and JET EFDA Contributors, Plasma Phys. Controlled Fusion **46**, 1877 (2004).

[8]C. Estrada-Mila, J. Candy, and R. E. Waltz, Phys. Plasmas **12**, 022305 (2005).
[9]C. Angioni, A. G. Peeters, F. Jenko, and T. Dannert, Phys. Plasmas **12**, 112310 (2005).
[10]F. Romanelli and S. Briguglio, Phys. Fluids B **2**, 754 (1990).
[11]H. Song and A. K. Sen, Phys. Fluids B **5**, 2806 (1993).
[12]J. W. Connor, R. J. Hastie, and P. Helander, Plasma Phys. Controlled Fusion **48**, 885 (2006).
[13]T. Antonsen, B. Coppi, and R. Englade, Nucl. Fusion **19**, 641 (1979).